Doublet Thermal Metadevice

Jiaxin Li,[1,2] Ying Li,[2] Tianlong Li,[1,3] Wuyi Wang,[1] Longqiu Li,[1,*] and Cheng-Wei Qiu[2,†]

[1] *State Key Laboratory of Robotics and System, Harbin Institute of Technology, Harbin 150001, China*

[2] *Department of Electrical and Computer Engineering, National University of Singapore, Singapore 117583, Singapore*

[3] *Department of Analytical, Physical and Colloidal Chemistry, Institute of Pharmacy, Sechenov University, Moscow 119991, Russia*

(Received 23 December 2018; revised manuscript received 2 February 2019; published 8 April 2019)

Thermal metamaterials have served as a practical way to manipulate heat flow thanks to their judiciously designed structures, which achieve various functionalities. However, the connection and interplay between various possible structural configurations and their functions' switchability have long been neglected and this is usually perceived as "one configuration, one function." Here, we propose a doublet thermal metadevice in which we utilize the local configuration of two unequal conductivity phases to manipulate global temperature distribution. Based on effective medium theory, we apply the phase interchange identity to show that the functionalities of transparency, cloaking, concentrating, and rotating can be unified. The doublet thermal metadevice is capable of realizing tunable multifunctions by simply adjusting the angular displacement of specific sublayers of the assembly. The functional diversity of the device can be further extended in two ways. One way is to use a secondary transformation and the other way is to alter the shape parameter of the unit phase. This work provides a different framework to understand and design thermal metamaterials, which might be extended to other disciplines such as optics, electromagnetics, and acoustics.

DOI: 10.1103/PhysRevApplied.11.044021

I. INTRODUCTION

Various types of thermal metamaterials or metadevices have been designed and realized based on the theory of transformation thermotics [1–8] or scattering cancellation [9–17], in order to achieve previously inconceivable thermal properties or functions such as thermal cloaking [1–4,9–13], thermal concentrating [2,13,14], thermal rotating [4,13], thermal converging [5], thermal transparency [15–17], and thermal illusion [6–8,17]. Recently, the controllability of the functionalities of thermal metamaterials has drawn a lot of research interest. The scheme of active metamaterials [18,19] has been proposed and thermoelectric components [19] have offered a method for actively controlling heat flux. Temperature-dependent transformation thermotics [20] has been developed and a series of alternative functional devices using nonlinear material have been demonstrated, such as a switchable thermal cloak [20], a switchable thermal concentrator [21], a thermal cloak–concentrator [22], and a temperature-trapping device [23]. The design of tunable multifunctional thermal metamaterials is realized by programmed reassembly of unit-cell thermal shifters [24]. However, tunable metamaterials with no need for altering their physical construction remain to be explored.

Here, an alternative method is used to design metadevices with doublet unequal thermal conductivity phases. It is well known that most thermal metamaterials are designed with anisotropic thermal conductivity, which is usually realized by alternating layered isotropic media, such as the layered structure of a cloak and the sensu-shaped structure of a concentrator. For traditional thermal metamaterials, once the structure is adopted, the function of the device is confined as designed because the anisotropic conductivity of alternating bulk materials cannot be adjusted after construction. Here, we discretize two unequal conductivity materials into unit cells and arrange the two phases in a staggered layout as a chessboardlike structure. Every movable sublayer consists of a string of two alternating phases, so the local conductivities in the two principle directions take variable values when the sublayers are rotated between each other. In this way, the local heat flux can be manipulated and the global temperature distribution can be switched.

Based on effective medium theory, we use duality relations to obtain the exact formula for the effective conductivity of a two-phase thermal conducting medium. By applying the phase interchange identity, we demonstrate

*longqiuli@hit.edu.cn
†chengwei.qiu@nus.edu.sg

that the design theory of thermal transparency, cloaking, concentrating, and rotating can be unified into the same framework. We develop a tunable metadevice that enables the realization of multiple functions with the same assembly but different configurations, and the functions can be switched by simply adjusting the angular displacement of specific sublayers. Then we provide two kinds of schemes using anisotropic phases through a second transformation or using isotropic phases by altering the shape parameter in order to extend the functional diversity of the device. We demonstrate the multiple functions of the proposed device in simulations. In contrast to previous approaches, our tunable doublet metadevice is expected to be freely controlled without out-of-plane deformation and rapidly adjustable without disassembly of constituting parts.

II. THEORETICAL ANALYSIS

Duality transformations were first applied to conductivity problems by Keller [25]. A phase interchange identity is obtained in binary periodic composites, which relates the effective conductivity of two-dimensional (2D) microgeometries of two isotropic phases with that of the reciprocal system obtained by interchanging its constituent materials. The relation is that the macroscopic effective conductivity along a principal direction is proportional to the inverse of the conductivity along the orthogonal direction of the reciprocal system, and the proportionality constant is the product of the conductivities of two constituent materials. Then this result, known as Keller's theorem, is generalized to a general form [26] and locally anisotropic 2D composites [27]. Special cases are discussed and some applications have been developed [28,29]. Although Keller's theorem was originally presented in terms of electric conductivity, it also holds in other problems governed by Laplace's equation, such as the dielectric permittivity, the elastic moduli, or the thermal conductivity [29]. A vital theme in the derivations of duality relations is that a curl-free field (e.g., an electrostatic field or a thermal gradient) produces a divergence-free field (e.g., an electric current or a heat flux), when the 2D system is rotated pointwise by 90°, and vice versa, so that a rotated excitation (response) field in the 2D system may be interpreted as the response (excitation) field for its reciprocal system. Detailed derivation of the reciprocal theorem is provided in the Supplemental Material [30].

Here, we rewrite Keller's theorem in the terms of thermal conductivity. For a series of symmetric materials, interchanging the two phases has no effect on the properties of the material. Hence, this means that the two kinds of constituent phases are completely equivalent. The effective conductivity tensor κ^* is related to the conductivities of constituent materials κ_1 and κ_2 of the system by

$$\det \kappa^* = \kappa_1 \kappa_2. \tag{1}$$

In Cartesian coordination, the effective thermal conductivities in the x and y directions (κ_x^* and κ_y^*) are related by $\kappa_x^* \kappa_y^* = \kappa_1 \kappa_2$. A special example of such a symmetric material, which is isotropic as far as its effective conductivity, is a chessboard. Then Eq. (1) immediately gives $\kappa^* = \sqrt{\kappa_1 \kappa_2}$, which means the macroscopic effective conductivity is given simply by the geometrical mean of the conductivities of its two phases. Imagine a chessboard composed of two unequal conductivity materials κ_1 and κ_2, surrounded by the background $\kappa_0 = \sqrt{\kappa_1 \kappa_2}$. If we extract the high-conductivity phase placed in the background, a diffusion effect on the temperature gradient is shown in Fig. 1(a), while the low-conductivity phase, which is now alone embedded in the background, exhibits a concentrating effect on the temperature gradient as shown in Fig. 1(b). Combining the two phases into a chessboard structure, we obtain a neutral temperature gradient and an effective conductivity equal to that of the background as in Fig. 1(c).

In polar coordination, Eq. (1) can be written in the form as follows:

$$\kappa_r^* \kappa_\theta^* = \kappa_1 \kappa_2, \tag{2}$$

where κ_r^* and κ_θ^* are the effective thermal conductivities in the radial and tangential directions, respectively. The counterpart of a chessboard in polar coordination is shown in Fig. 1(d). If the two-phase structure in polar coordination is macroscopically isotropic just as the chessboard in Cartesian coordination, which means that the effective conductivities in radial and tangential directions satisfy $\kappa_r^* = \kappa_\theta^*$, we need to hold $\ln(r_{i+1}/r_i) = \Delta\theta$, where $\Delta\theta$ is the central angle of a unit phase and r_i ($i = 1,2,\ldots,n$) is the inner radius of the ith annular layer of the structure.

The 2D geometry structure shown in Fig. 1(d) forms a macroscopically homogenous and isotropically hollow cylinder. Imagine every annular layer of the device is movable and rotatable. Here, we consider the ideal case, which ignores all the thermal resistances of the interfaces. If we keep the odd-numbered layers at their original locations and rotate the even-numbered layers in Fig. 1(d) by the central angle of a unit phase $\Delta\theta$, we obtain a structure with the same kind of material aligned along the radial direction as shown in Fig. 1(e). On the basis of the structure shown in Fig. 1(e), if we fix the 1st (5th, 9th) layer, continue to rotate the 2nd (6th, 10th) layer by $\Delta\theta/2$, rotate the 3rd (7th, 11th) layer by $\Delta\theta$, and rotate the 4th (8th, 12th) layer by $3\Delta\theta/2$, then we have the structure shown in Fig. 1(f). No matter by which angle each layer is rotated, Keller's theorem holds and the relation $\kappa_r^* \kappa_\theta^* = \kappa_1 \kappa_2$ exists.

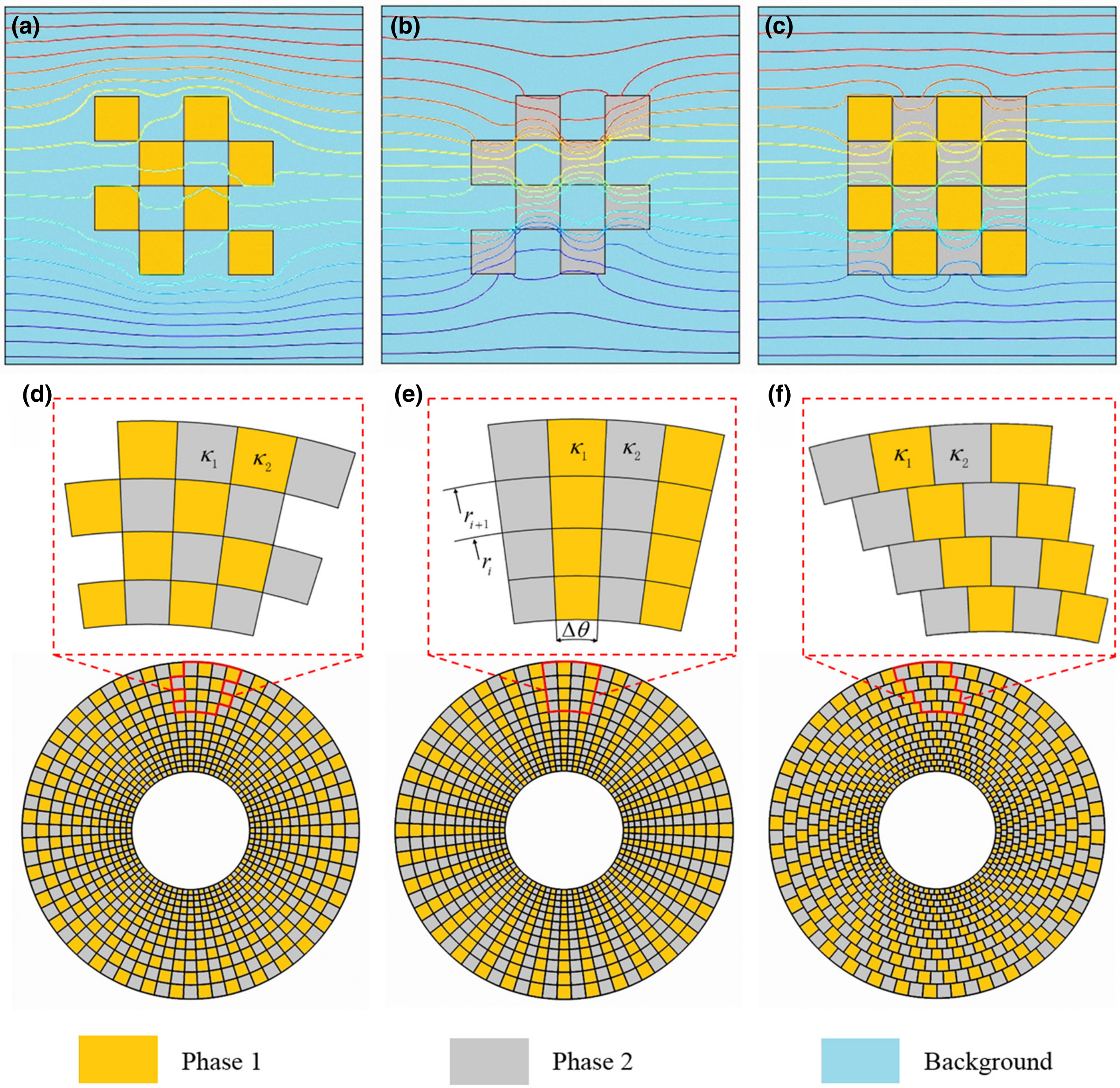

FIG. 1. Structures with two equivalent phases. Diagram of periodic structure of a chessboard in (a)–(c) Cartesian coordination and (d)–(f) polar coordination. Isothermal lines in (a)–(c) exhibit the effect of different conductive phases on the temperature profile. (d)–(f) illustrate the configurations of the device at the modes of transparency, concentration, and rotation, respectively.

Then we introduce the application of Keller's theorem in the design of a multifunctional thermal device. First, we consider a hollow cylinder with anisotropic thermal conductivity tensor $\kappa_c = \mathrm{diag}(\kappa_r, \kappa_\theta)$ embedded in an isotropic background material κ_0. Considering the structure placed in a uniform thermal gradient field without internal heat sources, the steady-state conduction equation satisfies the Laplace equation

$$\nabla \cdot (-\kappa \cdot \nabla T) = 0. \tag{3}$$

By variable separation, we obtain the expression of Eq. (3) in polar coordinates

$$\frac{1}{r}\frac{\partial}{\partial r}\left(r\kappa_r\frac{\partial T}{\partial r}\right) + \frac{1}{r}\frac{\partial}{\partial \theta}\left(\frac{\kappa_\theta}{\theta}\frac{\partial T}{\partial r}\right) = 0. \tag{4}$$

For the anisotropic cylinder embedded in backgrounds with thermal conductivity κ_0, the condition $\kappa_r\kappa_\theta = \kappa_0^2$ ensures that the external thermal flux is kept undistorted [9,14,16], that is, the temperature mismatch in the external regime is cancelled out at the interfaces of thermal metamaterials and the external environments.

As far as our periodic structure of two isotropic phases shown in Figs. 1(g)–1(i), the phase interchange identity gives $\kappa_r^*\kappa_\theta^* = \kappa_1\kappa_2$. We set $\kappa_1\kappa_2 = \kappa_0^2$, which gives $\kappa_r^*\kappa_\theta^* = \kappa_0^2$, so that the external thermal flux remains undistorted during the changing of the configuration of the geometric structure. But the value of $\kappa_r^*/\kappa_\theta^*$ makes a difference in the thermal gradient inside the hollow cylinder. The multifunctional device can be designed based on the following criteria. Namely,

(1) When $\kappa_r^* = \kappa_\theta^*$, as shown in Fig. 1(d), the structure serves as a thermal transparency device.

(2) When $\kappa_r^* > \kappa_\theta^*$, as shown in Fig. 1(e), the structure serves as a thermal concentrator.

(3) When $\kappa_r^* > \kappa_\theta^*$, if we rotate the anisotropic conductivity tensor $\mathrm{diag}(\kappa_r, \kappa_\theta)$ by a rotation matrix $\mathbf{R}$, the structure serves as a thermal rotator. The rotation matrix $\mathbf{R}$ is denoted as follows

$$\mathbf{R} = \begin{bmatrix} \cos\beta & -\sin\beta \\ \sin\beta & \cos\beta \end{bmatrix},$$

where β can be roughly calculated by $\beta = \arctan\{\Delta\theta/[2(e^{\Delta\theta} - 1)]\}$ for the structure [see Fig. 1(f)].

(4) When $\kappa_r^* < \kappa_\theta^*$, the structure serves as a thermal cloak. The effect of the cloak especially tends to be perfect when $\kappa_r^*/\kappa_\theta^* \to 0$.

Although the structures shown in Figs. 1(d)–1(f) cannot act as a cloak through rotating several layers of the device, we can still achieve the cloak function by using two kinds of anisotropic phases through a second transformation or by changing the shape of the unit phase, which is explained in detail in the next section.

III. RESULTS

A. Doublet metadevice with two isotropic phases

First, without loss of generality, we take a hollow cylinder consisting of 12 sublayers with each layer divided into 72 fan-shape unit cells as an example to validate the proposed scheme. Two kinds of isotropic materials are alternately aligned in every annular layer, which can be rotated freely [see Figs. 2(a), 2(d), and 2(g)]. The thermal conductivities of phase 1, phase 2, and the background materials are defined as $\kappa_1 = 20$ W/(K · m), $\kappa_2 = 0.05$ W/(K · m), and $\kappa_0 = 1$ W/(K · m), respectively. Here, we choose the parameters $r_1 = 4.5$ cm and r_i ($i = 2,3,\ldots,13$) as calculated by the formula $\ln(r_{i+1}/r_i) = \Delta\theta$.

On the premise of neglecting the thermal resistance at all the interfaces, full-wave simulations are carried out in a commercial software, COMSOL MULTIPHYSICS. In the simulation set up, the computational domain is a square with a side length of 40 cm. The top and bottom sides of the computational domain are set as fixed temperatures of 373 and 273 K, respectively, while the left and right sides take insulation boundary conditions.

We first examine the performance of thermal transparency in the chessboardlike configuration [see Fig. 2(a)]. The corresponding simulated temperature distribution is shown in Fig. 2(b). It is noted that when the device is at the mode of transparency, the radial effective conductivity $\kappa_{\mathrm{tra},r}^*$ and the tangential effective conductivity $\kappa_{\mathrm{tra},\theta}^*$ are equal to that of the background κ_0. Therefore, the temperature distribution outside and inside the device is undistorted as nothing is there except for some local perturbations around the boundaries of the discrete units. Figure 2(c) shows the result of a theoretical reference model, which comprises the background material in both the interior and exterior of the annulus, with the annular material given the theoretical effective thermal conductivity of the device. Here, the temperature distribution is uniform with straight isothermal lines [see Fig. 2(c)].

We then investigate the performances of a thermal concentrator and a thermal rotator. Figures 2(d) and 2(g) present the configurations of the concentrator and the rotator, respectively. The corresponding simulated temperature profiles and isothermal lines are illustrated in Figs. 2(e) and 2(h), respectively. The simulation reveals the properties of the proposed tunable device, namely, no external distortion exists and the internal temperature gradient varies with the layout of the device. For example, a much greater internal gradient is observed in Fig. 2(e), while a rotated internal gradient is observed in Fig. 2(h). Similarly, results of theoretical reference models with the annular material given the macroscopically anisotropic effective conductivity are shown in Figs. 2(f) and 2(i). For the concentrator in Fig. 2(f), the effective conductivity is calculated by effective medium theory $\kappa_{\mathrm{con},r}^* = (\kappa_1 + \kappa_2)/2, \kappa_{\mathrm{con},\theta}^* = 2\kappa_1\kappa_2/(\kappa_1 + \kappa_2)$. As for the rotator shown in Fig. 2(i), the effective conductivity is calculated by $\kappa_{\mathrm{rot}}^* = \mathbf{R}\kappa_{\mathrm{con}}^*\mathbf{R}^T$.

B. Transformation-based metadevice with anisotropic phases

To add the cloak function into our doublet metadevice, we introduce the method of transformation thermotics. Compressing every unit phase along the radial direction (see Fig. 3), the transformation equations can be expressed as

$$\Delta r_i' = k\Delta r_i, \quad \Delta\theta' = \Delta\theta, \tag{5}$$

where $\Delta r_i = r_{i+1} - r_i$ and $k < 1$. Note that the material parameters in the transformed space can be expressed as

$$\kappa' = \frac{\mathbf{\Lambda}\kappa\mathbf{\Lambda}^T}{\det\mathbf{\Lambda}}, \tag{6}$$

where $\mathbf{\Lambda} = \partial(x', y', z')/\partial(x, y, z)$ is the Jacobian transformation matrix.

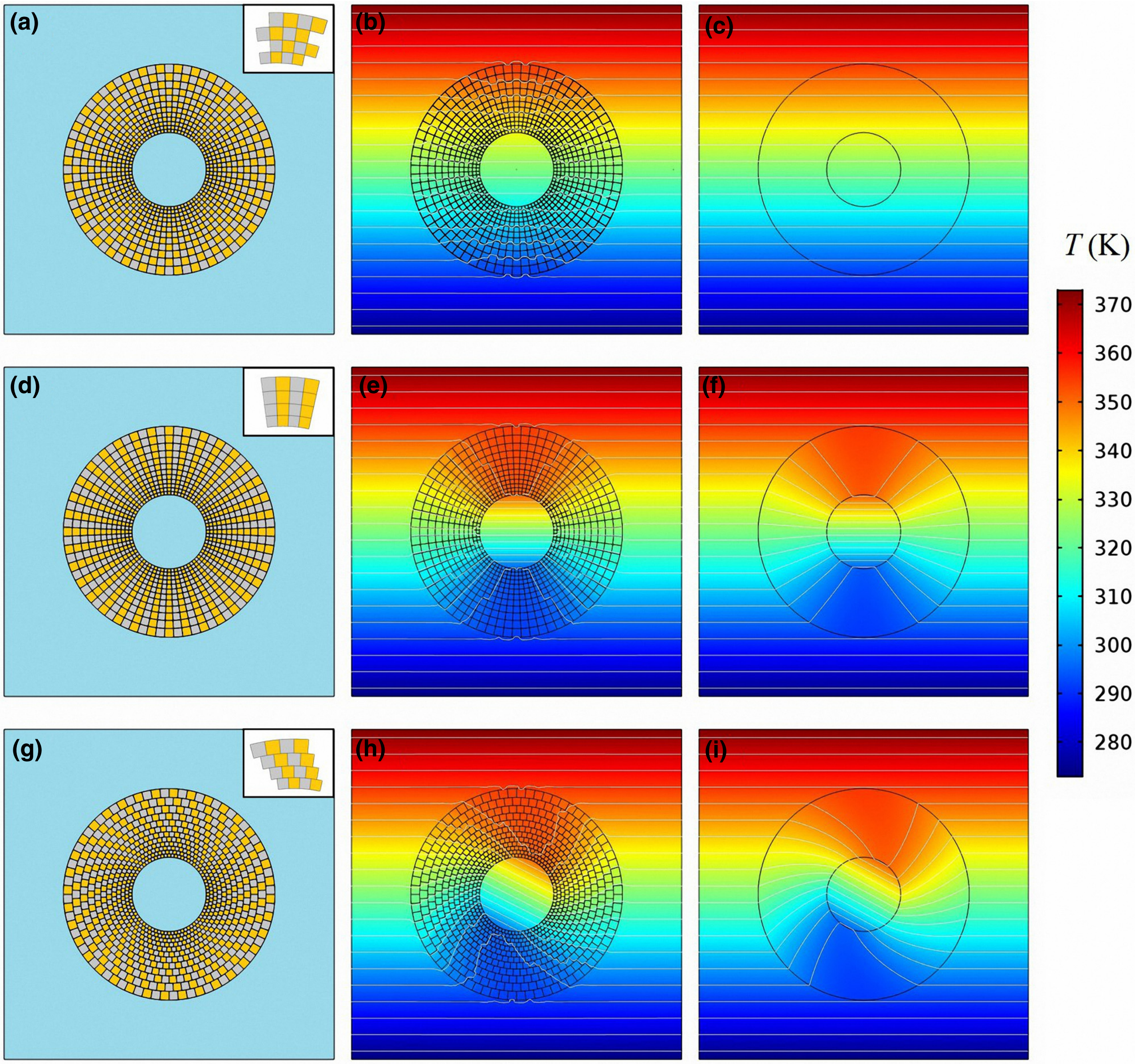

FIG. 2. Schemes of thermal devices with isotropic phases and corresponding simulated performances and comparison simulations, (a)–(c) thermal transparency, (d)–(f) thermal concentrator, (g)–(i) thermal rotator.

Then for each unit phase of conductivity κ_1 and κ_2, we have the corresponding conductivity after transformation

$$\kappa_1' = \begin{bmatrix} k\kappa_1 & 0 \\ 0 & \kappa_1/k \end{bmatrix}, \quad \kappa_2' = \begin{bmatrix} k\kappa_2 & 0 \\ 0 & \kappa_2/k \end{bmatrix}. \tag{7}$$

According to Keller's theorem, the structure resembling a chessboard shown in Fig. 3(a) is macroscopically homogenous with an isotropic effective conductivity $\kappa^* = \sqrt{\kappa_1\kappa_2}$. Then we have the transformed effective conductivity shown in Fig. 3(b)

$$\kappa^{*\prime} = \begin{bmatrix} k\sqrt{\kappa_1\kappa_2} & 0 \\ 0 & \sqrt{\kappa_1\kappa_2}/k \end{bmatrix}. \tag{8}$$

Note that $\det\kappa^{*\prime} = \kappa_1\kappa_2$ still exists after transformation. Then we can constitute a thermal cloak for we have $\kappa_r^{*\prime} < \kappa_\theta^{*\prime}$ after transformation. Similarly, we can calculate the transformed effective thermal conductivity of the structures under different configurations.

Then, we examine the performance of the doublet metadevice consisting of two kinds of anisotropic materials. The device can be rotated to shift among four functions: cloaking, concentrating, rotating, and transparency, as illustrated in Figs. 4(a), 4(d), 4(g), and 4(j), respectively. The device is assembled from 13 rotating sublayers, with each layer divided into 24 fan-shape unit cells. Two kinds of anisotropic materials are alternately arranged whose

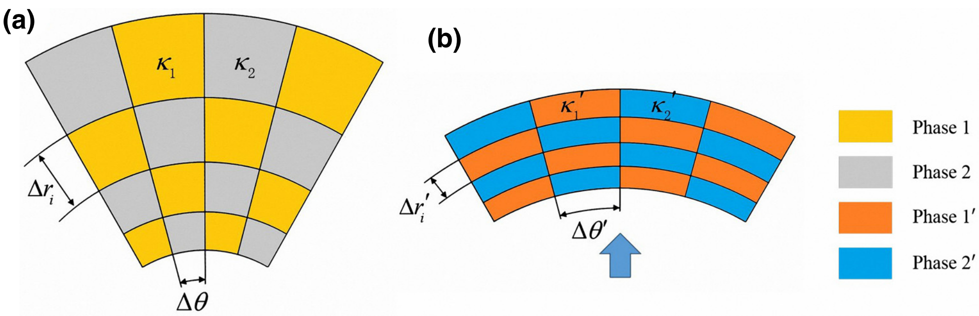

FIG. 3. Schematic of coordinate transformation along the radial direction for a chessboard structure. (a) Original space. (b) Transformed space.

conductivities are calculated from Eq. (7) through compression transformation, as illustrated in Fig. 3. Here, we take the compression proportionality coefficient k as $k = 1/\sqrt{10}$. Then the thermal conductivities of phase $1'$, phase $2'$, and background materials are defined as $\kappa'_{r1} = 2\sqrt{10}$ W/(K $\cdot$ m), $\kappa'_{\theta 1} = 20\sqrt{10}$ W/(K $\cdot$ m), $\kappa'_{r2} = 0.005\sqrt{10}$ W/(K $\cdot$ m), $\kappa'_{\theta 2} = 0.05\sqrt{10}$ W/(K $\cdot$ m), and $\kappa_0 = 1$ W/(K $\cdot$ m), respectively. It is worth mentioning that the anisotropic phase can be obtained by alternately stacking two kinds of isotropic layers according to effective medium theory. We set the inner radius $r'_1 = 4$ cm and $r'_i (i = 2,3,\ldots,14)$ is calculated by the revised formula $\ln(r'_{i+1}/r'_i)/\Delta\theta' = k$.

The diagrams and performances of the locally anisotropic metadevice are summarized in Fig. 4. The left column shows the configurations of the device in four modes (cloak, concentrator, rotator, and transparency). The middle column shows the performances of the device under a uniform temperature gradient field using COMSOL MULTIPHYSICS software. The right column gives the reference of theoretical models with the annular material defined as the theoretical effective thermal conductivity of the device. As illustrated in Fig. 4(b), the isothermal lines bend around the cloaking region. The temperature inside the device is almost constant, with the isothermal lines outside exhibiting minimal disturbance, similar to the properties displayed by a thermal cloak. Figure 4(e) shows the performance of a weakened thermal concentrator compared to that constituted by two isotropic materials with thermal conductivities of 20 and 0.05 W/(K $\cdot$ m), but the concentrating property still exists. Figure 4(h) shows the performance of a thermal rotator achieved from the concentrator by rotating the angle of $\Delta\theta/2$ layer by layer. Here, the rotator exhibits a larger rotation effect due to the larger ratio of included angle to thickness of the unit. In addition, we obtain the function of thermal transparency by adjusting the relative positions of the annuli, as shown in Fig. 4(k). Similar performances are obtained between our simulations in Figs. 4(b), 4(e), 4(h), and 4(k) and the theoretical models in Figs. 4(c), 4(f), 4(i), and 4(l), with some inevitable local disturbance of the unsmooth isotherm lines.

C. Shape parameter-based doublet metadevice with isotropic phases

Finally, we propose another way to design the radial and tangential effective thermal conductivities of our device. For the device with interlaced phases like a chessboard, the shape of the unit phase can dominate its effective conductivity in two principle directions. We present the performances of the device as a function of the shape parameter $\eta = \ln(r_{i+1}/r_i)/\Delta\theta$, while the variation of η is shown in Fig. 5. The thermal conductivities of two isotropic phases and background materials are defined as $\kappa_1 = 20$ W/(K $\cdot$ m), $\kappa_2 = 0.05$ W/(K $\cdot$ m), and $\kappa_0 = 1$ W/(K $\cdot$ m). Structures of different unit shapes with η taking the values of 1/3, 1, and 3 are illustrated in Figs. 5(a)–5(c), respectively. Figures 5(d)–5(f) show the corresponding temperature profiles and we can see an analogous cloaking effect in Fig. 5(d) and a concentrating effect in Fig. 5(f). This means that we can also design the device with four functions (cloak, concentrator, rotator, and transparency) with only two kinds of isotropic materials when we choose a small value of η and repeat the above steps. Here, we propose a formula to estimate the effective thermal conductivity κ_r^* and κ_θ^* as a function of κ_1, κ_2 and η

$$\kappa_r^*(\kappa_1,\kappa_2,\eta) = \begin{cases} \sqrt{\kappa_1\kappa_2}\left[\left(1-\frac{2\sqrt{\kappa_1\kappa_2}}{\kappa_1+\kappa_2}\right)(\eta-1)+1\right], & \eta \le 1 \\ \frac{\sqrt{\kappa_1\kappa_2}}{\left(1-\frac{2\sqrt{\kappa_1\kappa_2}}{\kappa_1+\kappa_2}\right)\left(\frac{1}{\eta}-1\right)+1}, & \eta \ge 1 \end{cases},$$
$$\kappa_\theta^*(\kappa_1,\kappa_2,\eta) = \begin{cases} \frac{\sqrt{\kappa_1\kappa_2}}{\left(1-\frac{2\sqrt{\kappa_1\kappa_2}}{\kappa_1+\kappa_2}\right)(\eta-1)+1}, & \eta \le 1 \\ \sqrt{\kappa_1\kappa_2}\left[\left(1-\frac{2\sqrt{\kappa_1\kappa_2}}{\kappa_1+\kappa_2}\right)\left(\frac{1}{\eta}-1\right)+1\right], & \eta \ge 1 \end{cases}. \quad (9)$$

We then examine the derived formula by comparing the analytical results with those calculated by the finite element method, as illustrated in Fig. 5(g). Letting $C = \kappa_1/\kappa_2$, we verify the effectiveness of the derived formula when η and C take various values. The vertical axis represents the normalized effective conductivities obtained by

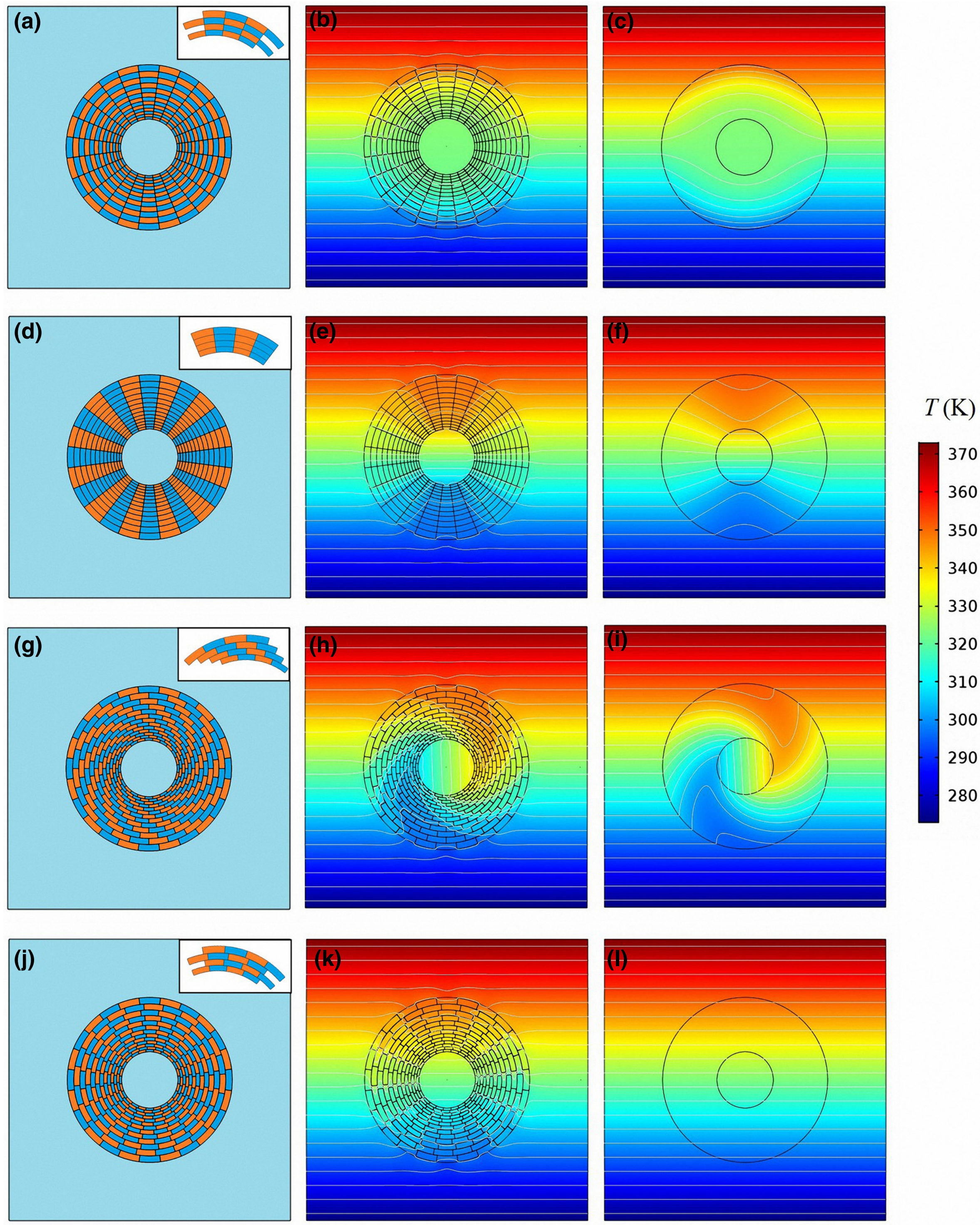

FIG. 4. Schemes of thermal devices with anisotropic phases and corresponding simulated performances and comparison simulations, (a)–(c) thermal cloak, (d)–(f) thermal concentrator, (g)–(i) thermal rotator, (j)–(k) thermal transparency.

dividing κ_r^* or κ_θ^* by $\sqrt{\kappa_1\kappa_2}$. The triangular and circular splashes in the graph exhibit the numerical results of radial and tangential effective conductivities calculated by COMSOL MULTIPHYSICS software, while the solid and dash lines represent the analytical results calculated by the proposed formula. Good agreement is obtained for the two sets of data shown in the graph, demonstrating the validity of our estimation formula.

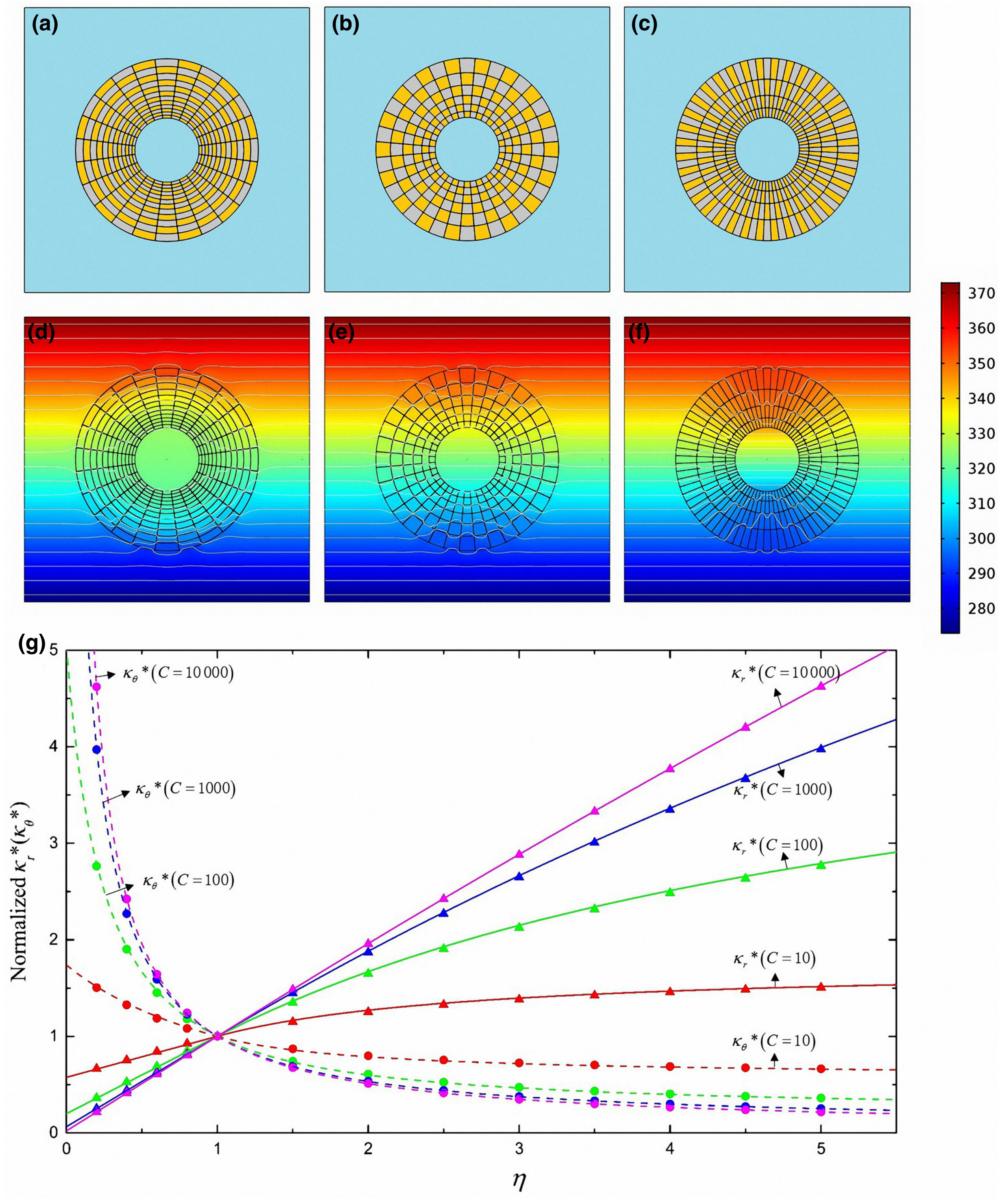

FIG. 5. Verification of anisotropic effective conductivities caused by geometric shape properties of the unit phase. Structure schemes: (a) $\eta = 1/3$, (b) $\eta = 1$, (c) $\eta = 3$. (d)–(f) are temperature distributions corresponding to (a)–(c). (g) Shows the relationship between the normalized thermal conductivity and the shape parameter η. The triangular and circular splashes exhibit the numerical results, while the solid and dash lines represent the analytical results.

In practice, our model can be realized by assembling a group of concentric cylinder shells, and the switching process can be implemented by applying torque to each part through proper design of the transmission mechanism. In reality, the contact interface in a realistic thermal device is inevitable, under which condition the thermal contact interface would degrade the predesigned performance of the device. Thus the interface resistance between sublayers should be considered as a design factor. The effect of interface resistances on the performance of a metadevice is discussed in the Supplemental Material [30]. The thermal resistance highly depends on the surface topography of the interfaces and the fit modes of the parts. An interference fit can reduce the contact thermal resistance, but causes an increasing driving torque. A clearance fit is more beneficial to drive movable parts, and we could choose a proper thermal compound whose conductivity is matched with the environment as the lubricating material to compensate for the contact thermal resistance.

We point out that the approach is limited to situations with rotational symmetry in 2D, that is, the cylindrical geometry. However, a vital design concept in the doublet metadevice is that the local conductivities in two principle directions take variable values when the movable layers are rotated, and then the local heat flux can be manipulated. This design can also be applied in a doublet flat plate construction in one dimension. If the concentric annuli are replaced by parallel straight lines, we can attain a plate with a wide range of variable thermal conductivities that would be expected to serve as a continuously tunable thermal switch. The implementation of switching in a real device is much easier in a one-dimensional (1D) system.

IV. CONCLUSION

In summary, based on the phase interchange identity, we propose an advanced method for the design of a doublet metadevice with homogenous two-phase material, which can be rotated to shift among different functions. We further provide two schemes to enrich the versatility of the thermal device and demonstrate that such a metadevice can be realized with only two kinds of isotropic or anisotropic materials arranged in a layered annular configuration. The assembly of sublayers with two phases spaced around the ring enables four significant functions of thermal metamaterials, including cloaking, concentrating, rotating, and transparency. The proposed device exhibits good performances in different modes. This tunable doublet metadevice can become a promising candidate for further enhancement of manufacturability for its diverse functions with only a change in alignment. The scheme presented here paves a way to actively control thermal energy through different media, and also provides inspiration to design more varieties of controllable metadevices, such as concentrators (cloaks) with the tunable concentrating (cloaking) efficiency, rotators with the tunable rotation angle, and so on.

ACKNOWLEDGMENTS

The authors would like to acknowledge the financial support by the Shanghai Aerospace Science and Technology Innovation Fund (Grant No. SAST2016023), the PetroChina Innovation Foundation (Grant No. 2018D-5007-0305) and the National Natural Science Foundation of China (Grants No. 61671044, No. 61571031, No. 51705108, No. 91648201, and No. 51675140). J.L. acknowledges the China Scholarship Council (CSC) for financial support.

[1] C. Z. Fan, Y. Gao, and J. P. Huang, Shaped graded materials with an apparent negative thermal conductivity, Appl. Phys. Lett. **92**, 251907 (2008).

[2] S. Guenneau, C. Amra, and D. Veynante, Transformation thermodynamics: Cloaking and concentrating heat flux, Opt. Express **20**, 8207 (2012).

[3] R. Schittny, M. Kadic, S. Guenneau, and M. Wegener, Experiments on Transformation Thermodynamics: Molding the Flow of Heat, Phys. Rev. Lett. **110**, 195901 (2013).

[4] L. L. Zhou, S. Y. Huang, M. Wang, R. Hu, and X. B. Luo, While rotating while cloaking, Phys. Rev. A **383**, 759 (2019).

[5] X. Y. Shen, C. R. Jiang, Y. Li, and J. P. Huang, Thermal metamaterial for convergent transfer of conductive heat with high efficiency, Appl. Phys. Lett. **109**, 402 (2016).

[6] S. L. Zhou, R. Hu, and X. B. Luo, Thermal illusion with twinborn-like heat signatures, Int. J. Heat Mass Transf. **127**, 607 (2018).

[7] R. Hu, S. L. Zhou, Y. Li, D. Y. Lei, X. B. Luo, and C. W. Qiu, Illusion thermotics, Adv. Mater. **30**, 1707237 (2018).

[8] Y. Li, X. Bai, T. Z. Yang, H. L. Luo, and C. W. Qiu, Structured thermal surface for radiative camouflage, Nat. Commun. **9**, 273 (2018).

[9] T. C. Han, T. Yuan, B. Li, and C. W. Qiu, Homogenous thermal cloak with constant conductivity and tunable heat localization, Sci. Rep. **3**, 1593 (2013).

[10] T. C. Han, X. Bai, D. L. Gao, J. T. L. Thong, B. W. Li, and C. W. Qiu, Experimental Demonstration of a Bilayer Thermal Cloak, Phys. Rev. Lett. **112**, 054302 (2014).

[11] H. Y. Xu, X. H. Shi, F. Gao, H. D. Sun, and B. L. Zhang, Ultrathin Three-Dimensional Thermal Cloak, Phys. Rev. Lett. **112**, 054301 (2014).

[12] Y. Li, K. J. Zhu, Y. G. Peng, W. Li, T. Yang, H. X. Xu, H. Chen, X. F. Zhu, S. Fan, and C. W. Qiu, Thermal metadevice in analogue of zero-index photonics, Nat. Mater. **18**, 48 (2019).

[13] S. Narayana and Y. Sato, Heat Flux Manipulation with Engineered Thermal Materials, Phys. Rev. Lett. **108**, 214303 (2012).

[14] T. C. Han, J. Zhao, T. Yuan, D. Y. Lei, B. Li, and C. W. Qiu, Theoretical realization of an ultra-efficient thermal-energy harvesting cell made of natural materials, Energy Environ. Sci. **6**, 3537 (2013).

[15] X. He and L. Z. Wu, Thermal transparency with the concept of neutral inclusion, Phys. Rev. E **88**, 033201 (2013).

[16] R. Z. Wang, L. J. Xu, Q. Ji, and J. P. Huang, A thermal theory for unifying and designing transparency, concentrating and cloaking, J. Appl. Phys. **123**, 115117 (2018).

[17] T. Z. Yang, X. Bai, D. L. Gao, L. Z. Wu, B. W. Li, J. T. L. Thong, and C. W. Qiu, Invisible sensors: Simultaneous sensing and camouflaging in multiphysical fields, Adv. Mater. **27**, 7752 (2015).
[18] C. W. Lan, K. Bi, Z. H. Gao, B. Li, and J. Zhou, Achieving bifunctional cloak via combination of passive and active schemes, Appl. Phys. Lett. **109**, 1777 (2016).
[19] D. M. Nguyen, H. Y. Xu, Y. M. Zhang, and B. L. Zhang, Active thermal cloak, Appl. Phys. Lett. **107**, 016623 (2015).
[20] Y. Li, X. Y. Shen, Z. H. Wu, J. Y. Huang, Y. X. Chen, Y. S. Ni, and J. P. Huang, Temperature-Dependent Transformation Thermotics: From Switchable Thermal Cloaks to Macroscopic Thermal Diodes, Phys. Rev. Lett. **115**, 195503 (2015).
[21] Y. Li, X. Y. Shen, J. P. Huang, and Y. S. Ni, Temperature-dependent transformation thermotics for unsteady states: Switchable concentrator for transient heat flow, Phys. Lett. A **380**, 1641 (2016).
[22] X. Y. Shen, Y. Li, C. Jiang, Y. Ni, and J. P. Huang, Thermal cloak-concentrator, Appl. Phys. Lett. **109**, 031907 (2016).
[23] X. Y. Shen, Y. Li, C. R. Jiang, and J. P. Huang, Temperature Trapping: Energy-Free Maintenance of Constant Temperatures as Ambient Temperature Gradients Change, Phys. Rev. Lett. **117**, 055501 (2016).
[24] G. Park, S. Kang, H. Lee, and W. Choi, Tunable multifunctional thermal metamaterials: Manipulation of local heat flux via assembly of unit-cell thermal shifters, Sci. Rep. **7**, 41000 (2017).
[25] J. B. Keller, A theorem on the conductivity of a composite medium, J. Math. Phys. **5**, 548 (1964).
[26] K. S. Mendelson, A theorem on the effective conductivity of a two-dimensional heterogeneous medium, J. Appl. Phys. **46**, 4740 (1975).
[27] J. Nevard and J. B. Keller, Reciprocal relations for effective conductivities of anisotropic media, J. Math. Phys. **26**, 2761 (1985).
[28] A. Dykhne, Conductivity of a two-dimensional two-phase system, Sov. Phys. JETP **32**, 63 (1971).
[29] K. Schulgasser, A reciprocal theorem in two-dimensional heat transfer and its implications, Int. J. Heat Mass Transf. **19**, 639 (1992).
[30] See Supplemental Material at http://link.aps.org/supplemental/10.1103/PhysRevApplied.11.044021 for a proof of the reciprocal theorem and simulations of a realistic metadevice with contact interfaces.